Trop J Nat Prod Res, July 2025; 9(7): 3360 - 3370 **ISSN 2616-0684 (Print)**
ISSN 2616-0692 (Electronic)

Tropical Journal of Natural Product Research

Available online at https://www.tjnpr.org

Original Research Article

Characterization and *In Vitro* Evaluation of Silver Nanoparticles Synthesized from *Ficus deltoidea* for Wound Closure and Skin Regeneration

Retno Aryani[1], Erin Maytari[2], Hetty Manurung[3], Rudy A. Nugroho[2]*, Rudianto Rudianto[4]

[1]*Animal Anatomy and Microtechnique Laboratory, Department of Biology, Faculty of Mathematics and Natural Sciences, Mulawarman University, Jl. Barong Tongkok No. 4 Gn. Kelua, Samarinda, Kalimantan Timur, Indonesia.*
[2]*Animal Physiology, Development, and Molecular Laboratory, Department of Biology, Faculty of Mathematics and Natural Sciences Mulawarman University, Jl. Barong Tongkok No. 4 Gn. Kelua, Samarinda, Kalimantan Timur, Indonesia.*
[3]*Plant Physiology and Development Laboratory, Department of Biology, Faculty of Mathematics and Natural Sciences, Mulawarman University, Jl. Barong Tongkok No. 4 Gn. Kelua, Samarinda, Kalimantan Timur, Indonesia.*
[4]*Postgraduate student of Department of Biology, Faculty of Mathematics and Natural Sciences, Mulawarman University, Jl. Barong Tongkok No. 4 Gn. Kelua, Samarinda, Kalimantan Timur, Indonesia.*

ARTICLE INFO

Article history:
Received 12 May 2025
Revised 04 June 2025
Accepted 14 June 2025
Published online 01 August 2025

ABSTRACT

Ficus deltoidea (*F. deltoidea*), a medicinal plant known for its antioxidant and regenerative properties, has shown therapeutic potential in wound care. However, the potential of silver nanoparticles synthesized from *F. deltoidea* (Fd-AgNPs) for enhancing wound healing remains underexplored. This study evaluated topical ointments containing green-synthesized Fd-AgNPs at 10%, 20%, and 30% concentrations. The Fd-AgNPs were produced from *F. deltoidea* ethanolic leaf extract and characterized via UV–Vis spectrophotometry, scanning electron microscopy (SEM), Fourier transform infrared (FTIR) spectroscopy, and X-ray diffraction (XRD) analyses. Mice with full-thickness skin wounds received daily ointment treatments for 15 days. Wound healing progression was assessed through closure rates, histology, and biochemical markers, including protein content, hydroxyproline levels, total DNA, and fibroblast count. Among the treatments, 10% Fd-AgNP (T4) ointment resulted in complete wound closure by day 12 but yielded the lowest number of fibroblasts (1.58 ± 0.00) and substantial hydroxyproline content (3146.50 ± 79.54 µg/mL). Moreover, T5 (20%) presented higher protein (961.81 ± 90.67 µg/mL) and DNA levels (4.10 ± 0.15 µg/mL) than the other groups did, whereas T6 (30%) presented intermediate values for most markers (protein and DNA) between T4 and T5. Histological analysis confirmed improved tissue regeneration in mice treated with any concentration of Fd-AgNP topical ointment. These findings confirmed that Fd-AgNPs topical ointment enhances wound regeneration by promoting fibroblast proliferation and extracellular matrix synthesis. The study concluded that 20% Fd-AgNP ointment may offer an optimal equilibrium between healing velocity and quality, rendering it the most promising formulation for attaining both rapid and structurally robust wound healing.

Keywords: *Ficus deltoidea*, Silver nanoparticles, Green synthesis, Wound closure, Fibroblast, Hydroxyproline.

Introduction

Ficus deltoidea (*F. deltoidea*), a traditional medicinal herb formerly used to treat many diseases, shows great promise for use in wound healing.[1,2] *F. deltoidea* leaf extract contains many bioactive chemicals, including flavonoids, tannins, and alkaloids, all of which have notable antioxidant and anti-inflammatory properties.[3,4] Phytochemical investigations by Aryani[5] revealed notable phenolic compounds in *F. deltoidea* extract that enhance wound healing. Another *in vivo* study revealed that *F. deltoidea* extract enhances collagen production and fibroblast growth, which are crucial for wound healing.[6] Additionally, Raihandhany and Zen[2] reported that the topical application of *F. deltoidea* extract in a rat wound model significantly improved the wound closure rate and the regenerated tissue quality.

Wound healing is a comprehensive and dynamic biological process comprising a sequence of interconnected phases: hemostasis, inflammation, proliferation, and tissue remodeling.[7,8] During this process, diverse cell types, growth factors, cytokines, and extracellular matrix components interact in a coordinated fashion to restore the integrity of injured tissues.[9,10] Disruption in any phase can result in inefficient wound healing or the development of chronic wounds that are challenging to treat.[11]

Recent studies have indicated that good wound management relies not only on conventional care but also on new strategies that can expedite healing and prevent problems such as infection.[12] The demand for improved wound healing techniques has prompted the advancement of diverse therapeutic options, such as the application of nanotechnology in drug delivery systems, medicine,[13] and biomaterials that facilitate tissue regeneration.[14-16]

Nanotechnology, especially the application of silver nanoparticles (AgNPs), has emerged as a significant advancement in the field of wound healing.[16-18] These nanoparticles are valuable in the biomedical field because of their strong antimicrobial capabilities and their ability to modulate immune responses.[19-21] Their unique characteristics, such as a high surface-area-to-volume ratio and increased chemical activity,

*Corresponding author. Email: rudyagung.nugroho@fmipa.unmul.ac.id; Tel: +6281283088955

Citation: Aryani R, Maytari E, Manurung H, Nugroho RA, Rudianto R. Characterization and *In Vitro* Evaluation of Silver Nanoparticles Synthesized from *Ficus deltoidea* for Wound Closure and Skin Regeneration. Trop J Nat Prod Res. 2025; 9(7): 3360 – 3370 https://doi.org/10.26538/tjnpr/v9i7.64

Official Journal of Natural Product Research Group, Faculty of Pharmacy, University of Benin, Benin City, Nigeria

enable more precise and effective interactions with microorganisms and cellular structures.[22,23] Recent studies have also indicated that AgNPs can act as antibacterial agents and promote tissue regeneration and angiogenesis, which are essential elements of the healing process.[24,25] The manufacture of AgNPs via green methods employing plant extracts has garnered interest for its environmentally sustainable approach and promising ability to yield nanoparticles with enhanced biocompatibility,[26,27] primarily due to the role of bioreductants—phytochemicals such as flavonoids, polyphenols, and tannins in plant extracts—that reduce silver ions (Ag^+) to metallic nanoparticles (Ag^0) while simultaneously stabilizing them. For instance, the ethanolic extract of *F. deltoidea* leaves, rich in these bioreductants, facilitated the synthesis of AgNPs that demonstrated superior wound-healing properties *in vivo*.[5] Progress in analytical techniques and deeper insight into how AgNPs function have enabled the development of more effective formulations tailored for wound care.[17,28] Many scientific investigations have been dedicated to assessing the therapeutic effectiveness of AgNPs in wound healing. Research by Kar[29] indicated that hydrogels containing AgNPs could hasten wound healing in diabetic rat models by increasing growth factor expression and reducing oxidative stress. Another previous study demonstrated that wound dressings treated with AgNPs significantly inhibited several pathogens and promoted collagen formation in acute wound.[25] [30] Biologically produced AgNPs have been shown to have lower toxicity than their chemically manufactured equivalents while maintaining their therapeutic effectiveness. These findings were substantiated by a meta-analysis conducted by Yi[31], which demonstrated the significant effectiveness of AgNPs in improving wound healing results across different clinical settings.

Although earlier research has demonstrated the effectiveness of *F. deltoidea* in wound healing, AgNPs produced from *F. deltoidea* ethanolic leaf extract (Fd-AgNPs) have not been studied extensively. Few studies have investigated how the therapeutic qualities of *F. deltoidea* combine with the wound-healing properties of AgNPs.

This study's innovation lies in the application of *F. deltoidea* extract as a reducing agent and stabilizer in the synthesis of Fd-AgNPs, potentially yielding nanoparticles with enhanced biological activity. This green synthesis process provides a more sustainable and eco-friendly alternative to traditional synthesis techniques.[30,32] This research aimed to characterize Fd-AgNPs and assess their efficacy in wound healing via *in vivo* experiments in a mouse model. The physicochemical properties of the generated Fd-AgNPs were examined, including their particle size, shape, stability, and phytochemical content. Furthermore, the mechanism of action of Fd-AgNPs in wound healing was determined, and their viability as a therapeutic alternative for wound management was assessed.

Materials and Methods

Chemicals and Reagents

All chemicals utilized, such as silver nitrate ($AgNO_3$), sodium chloride (NaCl), phosphate-buffered saline (PBS), hydrochloric acid (HCl), and bovine serum albumin (BSA), were purchased from Sigma–Aldrich, Inc., USA, and were of analytical grade. All the solutions were produced with deionized water.

Collection and Identification of F. deltoidea Leaf

Dried *F. deltoidea* (Determination Certification Number: 12/07/23/Det/FMIPA, Faculty of Mathematics and Natural Sciences, Mulawarman University) was provided by a local farmer in Makroman village, District of Sambutan, East Kalimantan, Indonesia (0°21'18"-1°09'16" south; 116°15'36"-117°24'16" East). The *F. deltoidea* leaves were cut into small pieces and ground using a blender. The resulting plant material (2 kg) was subjected to maceration in 96% ethanol, and the mixture was stirred for 5 minutes daily. After 2 days, the extract was filtered through filter paper to separate the solid residue (leaf pulp) from the liquid filtrate. The filtrate was subsequently concentrated via a rotary evaporator at 50–60°C to remove ethanol, yielding a colloidal leaf extract.

Biosynthesis of Fd-AgNPs

The green synthesis of *F. deltoidea* silver nanoparticles (Fd-AgNPs) was conducted using 1 mM $AgNO_3$.[33] A total of 20 g of *F. deltoidea* ethanolic leaf extract was mixed with 200 mL of 96% ethanol at a ratio of 1:10. This solution was then mixed with 2000 mL of 1 mM $AgNO_3$, maintaining the same ratio (1:10). The combined mixture was thoroughly homogenized and incubated at 70°C for 30 hours. Upon completion, the resulting product was concentrated via a rotary evaporator. Successful nanoparticle formation was confirmed through visual observation of color transformation and the presence of the Tyndall effect, as described by standard characterization techniques.[34]

Characterization of Fd-AgNPs

The formation of Fd-AgNPs was determined via UV–visible spectrophotometry (Shimadzu UV-1280, Japan) by scanning across a spectral range of 350–750 nm. The surface topology and particle structure were examined by scanning electron microscopy (SEM; Hitachi SU 3500, Europe) at an accelerating voltage of 26 kV and a magnification of 50,000×. The crystalline structure and elemental composition were analyzed through X-ray diffraction (XRD; Bruker D8, Blue Scientific, USA) under operational settings of 40 kV and 35 mA, with a Cu Kα radiation wavelength of 1.54056 Å. Additionally, Fourier transform infrared (FTIR) spectroscopy (Agilent Cary 630, USA) was utilized to identify functional groups and bioactive compounds associated with the nanoparticle surface, following the procedure outlined by Das[35]

Formulation of Wound Ointment

The wound ointment was formulated with *F. deltoidea* ethanolic leaf extract, Fd-AgNPs, and Vaseline, following the composition outlined in Table 1. Initially, Vaseline was liquefied using a hot plate. Once fully melted, the *F. deltoidea* ethanolic leaf extract or the Fd-AgNPs were incorporated into the base. The mixture was continuously stirred until uniform consistency was achieved and then transferred into sterile ointment containers for storage and later application.[5]

Table 1: Wound ointment formula using Fd-AgNPs and Vaseline

Ingredients	Percentage (%)		
	10	**20**	**30**
Ficus deltoidea ethanolic leaf extract or Fd-AgNPs (g)	3	6	9
Vaseline (g)	27	24	21
Total (g)	30	30	30

Animal Preparation and Experimental Design

Ethical clearance for the use of laboratory animals in this in vivo wound healing investigation (totaling 72 mice) was granted by the Health Research Ethics Committee of the Faculty of Medicine, Mulawarman University, Samarinda, Indonesia (Approval No. 06/KEPK-FK/I/2023). All experimental procedures were carried out in alignment with the ARRIVE guidelines to ensure ethical and responsible animal research practices.

A total of 72 male mice (approximately 3 months old, with an average initial body weight of ±20 g) were obtained from a breeding facility in Samarinda, Indonesia. The mice were randomly allocated into 9 groups, 3 of which served as controls (C– (incision without treatment), C+Vas (incision treated with Vaseline), and C+Pov (incision treated with povidone-iodine) and 6 of which received the following treatments: groups T1–T3 were administered a wound ointment formulated with an ethanolic extract of *F. deltoidea* leaves at concentrations of 10, 20, and 30%, respectively, and groups T4–T6 were treated with a silver nanoparticle-based ointment (Fd-AgNPs) at the same respective concentrations. Each group included 8 mice. Prior to the experiment, all the animals underwent a 7-day acclimatization period under standard laboratory conditions with unrestricted access to food and water.

The mice were anesthetized via a 10% ketamine solution (0.2 mL, intramuscularly) prior to wound induction. Three minutes postinjection, the dorsal fur was shaved to expose the skin, which was subsequently disinfected with 70% ethanol. A linear incision measuring 1 cm in length and 1 mm in depth was made using a sterile scalpel. Treatments corresponding to each group were applied daily from day 0 to day 15. Wound healing was monitored by measuring wound closure on days 0, 3, 6, 9, 12, and 15 using a digital caliper. Photographic documentation of each wound was also obtained throughout the study. The percentage of wound closure was calculated every 3 days via the following formula:

$$Px = [\frac{p^2 - px^2}{p^2}] \times 100\%$$

Where;
Px represents the percentage of wound closure on day x,
p is the initial wound length (day 0),
px is the wound length on the specified day x.

On day 10, the mice in the groups with the most advanced healing were selected and anesthetized for tissue analysis. Skin tissue samples were harvested from the wound area and divided into four equal portions (0.05 g each). These samples were processed as follows: the first portion was mixed with 200 µL of 4% NaCl for protein analysis; the second portion was combined with 200 µL of PBS for DNA quantification; the third portion was incubated at 60°C overnight for hydroxyproline determination; and the fourth portion was preserved in 10% neutral buffered formalin for histological evaluation.

Protein Content Determination
The protein concentration in the wound tissue was assessed via a modified Lowry assay. Approximately 0.05 g of skin tissue from the wound area was weighed and placed into a microtube containing 200 µL of 4% NaCl solution. The sample was homogenized via a Beadbug Microtube Homogenizer (USA) at 3,000 rpm for 30 seconds. The homogenate was then centrifuged at 6,000 rpm for 10 minutes at ambient temperature. One hundred fifty microliters of the supernatant was transferred to a new tube and mixed with 1,200 µL of Lowry B reagent, followed by a 10-minute incubation at room temperature. Subsequently, 150 µL of Lowry A reagent was added, and the mixture was gently homogenized and incubated for an additional 20 minutes. A bluish coloration indicated the presence of protein, and the absorbance was measured at 600 nm via a UV–Vis spectrophotometer (UV–Vis 752 N, China). Bovine serum albumin (BSA) served as the standard for calibration.

Hydroxyproline Level Assessment
Wound tissue samples (0.05 g) were homogenized in 200 µL of phosphate-buffered saline (PBS) at 3,000 rpm for 30 seconds in preparation for hydroxyproline quantification. The samples were then hydrolyzed in 6N hydrochloric acid at 130°C for 4 hours. Following hydrolysis, the pH was adjusted to neutral (pH 7) via the oxidant Chloramine-T, and the mixture was allowed to react at room temperature for 20 minutes. The reaction was stopped by the addition of 0.4 M perchloric acid. Subsequently, Ehrlich's reagent was added, and the mixture was incubated at 60°C for 90 minutes. The resulting colorimetric change was measured at 557 nm via a UV–Vis spectrophotometer (UV–Vis 752N, China). A standard calibration curve was constructed using known hydroxyproline concentrations (0–400 µg/mL) processed identically to the samples.

Total DNA Evaluation
For the DNA analysis, total DNA was extracted from the same tissue samples via a Universal DNA Extraction Kit (D2100, Solarbio, Beijing). Quantification was performed via the Qubit™ dsDNA Assay Kit (Cat. No. Q32851; Thermo Fisher Scientific, USA), and measurements were read on a Qubit 4 fluorometer (Invitrogen, Thermo Fisher Scientific, USA).

Histological Preparation and Analysis
Skin tissue samples from the wound area of the mice were collected for histological evaluation on treatment day 10. Tissue processing was conducted per the standard paraffin embedding protocol, and the sections were stained with hematoxylin and eosin (H&E) for cellular structure visualization. Observations were conducted under a light microscope (Zeiss Primo Star, Germany) at 100× magnification. Fibroblast quantification was conducted on the basis of criteria adapted from a previously established method.[36]

Data Analysis
Characterization of the synthesized Fd-AgNPs is presented through descriptive graphs and micrographs. Quantitative data, including wound closure rates, protein content, hydroxyproline levels, total DNA, and fibroblast numbers, were statistically evaluated via SPSS software (version 22; SPSS Inc., Chicago, IL, USA). One-way ANOVA was used to detect significant differences among the treatment groups. When ANOVA indicated significance, Duncan's multiple range test (DMRT) was applied to identify specific group differences. All the results were interpreted at a significance level of $p < 0.05$.

Results and Discussion

Characterization of Fd-AgNPs
The Fd-AgNPs were synthesized and characterized using an eco-friendly green synthesis approach. The resulting nanoparticles were characterized via Tyndall effect observation, UV–Vis spectrophotometry, SEM, FTIR, and XRD analysis. Following successful synthesis confirmation, the wound-healing efficacy of various concentrations of AgNP-based ointments was evaluated in a mouse model. Biochemical, histological, and cellular assessments, including protein content, hydroxyproline level, DNA quantification, and fibroblast number, were performed to assess tissue regeneration and wound closure.
Present results displayed the Tyndall effect in three distinct samples: (a) 1 mM *F. deltoidea* ethanolic leaf extract, (b) 1 mM $AgNO_3$ solution, and (c) 1 mM Fd-AgNPs (Figure 1). A visible red laser beam was passed through each sample to detect the presence of colloidal particles through light scattering, a phenomenon known as the Tyndall effect. Sample (a), containing only the ethanolic extract, demonstrated a faint red-light line, indicating the presence of some dispersed phytochemical constituents but no significant colloidal activity. Meanwhile, sample (b), containing only silver nitrate solution, appeared transparent with no observable light scattering, consistent with the absence of particulate matter or nanoparticle formation. In contrast, sample (c), representing the synthesized Fd-AgNPs, clearly exhibited a bright, well-defined red path of the laser beam across the cuvette, indicating strong light scattering. The absence of light scattering in the $AgNO_3$ solution (b) confirmed that silver ions alone did not produce a colloidal system.[37,38] Moreover, the weak Tyndall effect observed in the pure *F. deltoidea* ethanolic leaf extract (a) may be attributable to phytoconstituents such as flavonoids, phenolics, and other organic compounds, which, while contributing to slight light scattering, are insufficient to cause a well-defined beam without nanoparticle synthesis.[39] This finding suggests the successful formation of a colloidal suspension of Fd-AgNPs. The difference in light scattering between the samples confirmed that the synthesis process altered the optical properties of the medium, consistent with nanoparticle generation.
The observed current results of Tyndall effects aligned with similar past findings regarding the green synthesis of AgNPs. For example, the Tyndall effect was used to verify nanoparticle formation in silver colloids synthesized with *Azadirachta indica* extract,[40] where only the nanoparticle sample showed a strong light path under laser exposure, comparable to the clear effect observed in sample (c). Additionally, previous research using *Moringa oleifera* leaf extract revealed similar results, indicating successful AgNPs formation due to phytochemical-mediated reduction and stabilization of silver ions.[41] These comparisons also confirmed that the *F. deltoidea* ethanolic leaf extract is an effective bioreductant and capping agent, forming well-dispersed Fd-AgNPs. The presence of bioactive molecules in *F. deltoidea*, including flavonoids and tannins,[42] likely plays a critical role in both the reduction of Ag^+ to Ag^0 and the stabilization of the nanoparticles in a colloid, as evidenced by the Tyndall effect.[43]

ISSN 2616-0684 (Print)
ISSN 2616-0692 (Electronic)

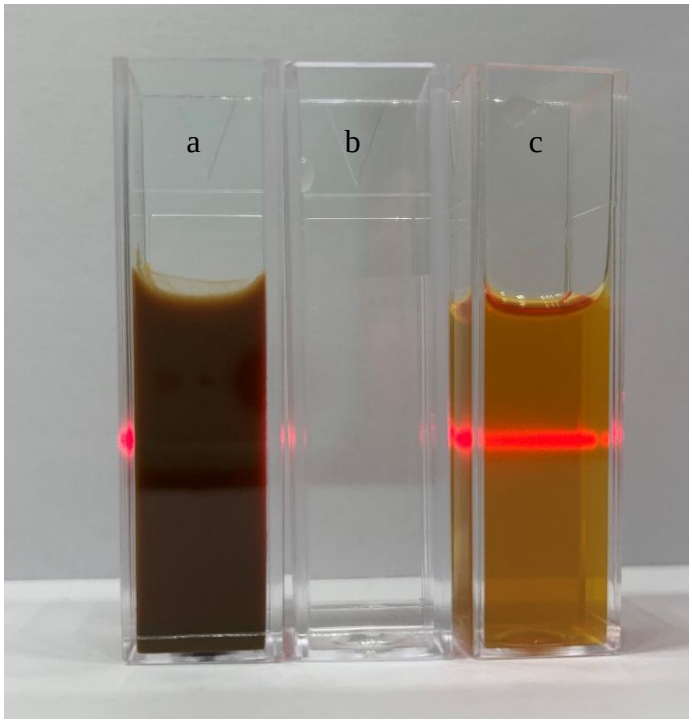

Figure 1: Tyndall effect of Fd-AgNPs. a) *Ficus deltoidea* ethanolic leaf extract 1mM, b) $AgNO_3$ 1 mM, c) Silver nanoparticle (AgNPs) synthesized using *Ficus deltoidea* ethanolic extract 1mM.

Furthermore, this result supports the growing body of evidence that green synthesis offers an environmentally friendly, cost-effective, and nontoxic route for nanoparticle production, with results comparable or superior to those obtained via conventional chemical synthesis methods.[44]

The UV–Vis absorption spectra of the *F. deltoidea* ethanolic leaf extract (orange curve) and Fd-AgNPs synthesized from the same extract (gray curve) are shown in Figure 2. The extract alone exhibited a broad absorption peak with a maximum absorbance near 525 nm, potentially corresponding to the presence of phytochemical constituents such as flavonoids, polyphenols, and other aromatic compounds.

The spectral profile changes significantly after adding silver nitrate before nanoparticle formation. The Fd-AgNP sample displayed a distinct, sharper absorbance peak centered at approximately 440–450 nm.[45] This peak is within the characteristic surface plasmon resonance (SPR) range of AgNPs, which typically appear between 400–450 nm depending on the particle size, shape, and medium. Compared with that of the extract spectrum, the absorbance of Fd-AgNPs at higher wavelengths (>500 nm) decreased more sharply, suggesting the formation of more uniform and smaller nanoparticles. The reduction in peak intensity beyond the SPR region indicated the completion of the reduction reaction and a decrease in nonmetallic or organic species from the plant extract in the nanoparticle suspension.

During the nanoparticle synthesis, bioactive compounds in the plant extract, such as polyphenols and flavonoids, act as reducing agents, converting silver ions (Ag^+) into metallic silver nanoparticles (Ag^0). This transformation is typically monitored using UV–Vis spectroscopy, where the emergence of a surface plasmon resonance (SPR) peak around 440 nm indicates the formation of AgNPs. As the reaction progresses and the reduction nears completion, a decrease in absorbance intensity beyond the SPR region is observed, signifying the consumption of organic compounds from the plant extract and the stabilization of the nanoparticles.[46]

In a recent study by Kantoma and Nwokem[47], AgNPs biosynthesized from *Calotropis procera* leaf extract presented an SPR peak at 437 nm, suggesting the presence of stable, spherical nanoparticles. Similarly, a peak at 445 nm was observed for the AgNPs synthesized from *Moringa oleifera*, which can be attributed to the narrowness and sharpness of the peak, the homogeneity of the particle size, and effective capping by plant phytochemicals.[48] These findings are consistent with those of the present study, where the sharp SPR peak at 440 nm for Fd-AgNPs suggests not only nanoparticle formation but also relatively good stability and dispersion,[49] possibly due to bioactive capping agents within the *F. deltoidea* ethanolic leaf extract. The initial absorbance spectrum of the *F. deltoidea* extract likely reflects the diverse range of secondary metabolites it contains. This plant is rich in flavonoids, saponins, and tannins, all of which can participate in reduction and stabilization processes during nanoparticle formation.[4,50] Moreover, the shift and change in spectral features upon nanoparticle synthesis provide indirect insight into the reaction kinetics and degree of completion. A clearly defined SPR band without additional peaks suggests that the majority of silver ions have been reduced, and no significant aggregation or secondary particle formation has occurred, which is favorable for downstream applications such as biomedical use.[51,52]

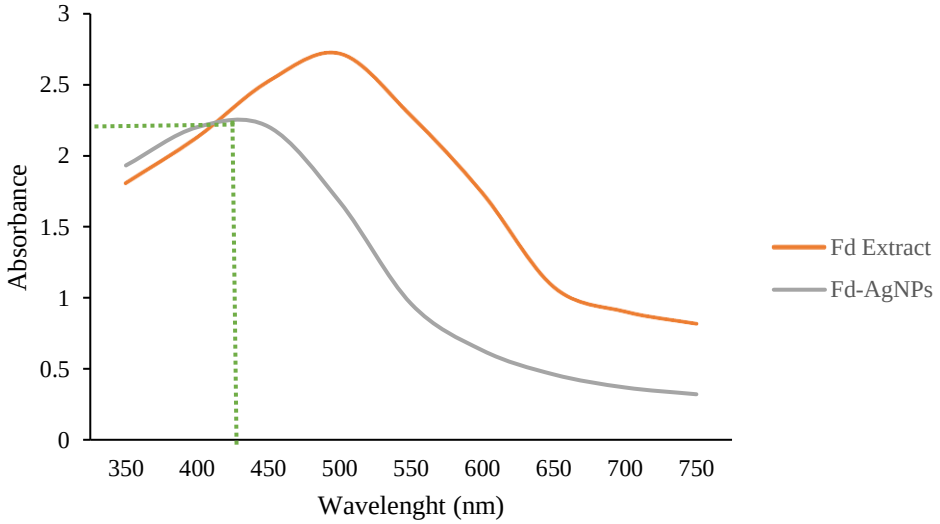

Figure 2: The UV-vis spectrophotometer (Absorbance) of *Ficus deltoidea* leaves ethanolic extract and silver nanoparticle (AgNPs) synthesized using ethanolic extract of *Ficus deltoidea* leaves

The SEM images of the Fd-AgNPs (Figure 3) revealed aggregated clusters of quasispherical nanoparticles of various sizes. The magnification at 20,000× revealed particles with irregular but predominantly spherical to oval morphologies distributed in dense agglomerates. While individual particles were visible, the Fd-AgNPs appeared fused or closely packed, likely due to surface adhesion and the natural tendency of the nanoparticles to form aggregates.

The estimated particle size was within the submicron range (<1 µm). Nanoparticles are tiny structures characterized by having at least one of their dimensions measuring between 1 and 100 nanometers, as per the International Organization for Standardization (ISO) and the National Nanotechnology Initiative (NNI).[53,54] More precise determination would require complementary techniques such as dynamic light scattering (DLS) or particle size analysis via ImageJ software. The observed aggregation and surface roughness suggest the presence of organic capping agents derived from *F. deltoidea* phytochemicals, which likely stabilize the nanoparticles during biosynthesis.

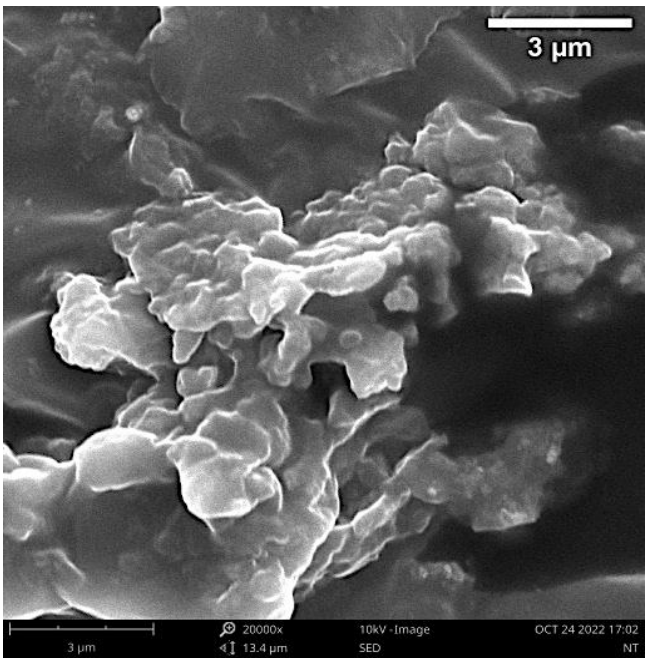

Figure 3: Scanning electron microscope (SEM) of AgNPs biosynthesized using *Ficus deltoidea* leaves extract

The surface texture appears rough, indicative of capping by bioactive compounds such as flavonoids, phenolic acids, and tannins, and functional groups were also confirmed by the FTIR data (e.g., OH and C=O stretching bands). These phytochemicals not only reduce Ag^+ ions to Ag^0 but also stabilize the nanoparticles, preventing uncontrolled growth and shape irregularities.[55,56] In contrast, the morphology of the Fd-AgNPs generated in the present study was irregular; in previous studies AgNPs synthesized from *Ocimum gratissimum* extract were monodispersed and uniform with no aggregation tendencies.[57] The relatively large and aggregated particle clusters identified in the present study could be attributed to the presence of multiple reducing and stabilizing compounds in *F. deltoidea*, which may promote both rapid nucleation and uncontrolled particle agglomeration. Nevertheless, the rough and coarse morphology may imply the potential for strong surface reactivity, which has been associated with enhanced antibacterial and wound healing properties *in vivo*. Furthermore, the FTIR spectrum of Fd-AgNPs (Figure 4) demonstrated a range of distinct absorption bands corresponding to various functional groups from the plant phytochemicals involved in the biosynthesis and stabilization of the nanoparticles. The broad and intense absorption peak observed at 3,383.91 cm^{-1} is attributed to O–H stretching vibrations, suggesting the presence of phenolic compounds or alcohol groups. The strong absorption at 2,918.97 cm^{-1} and 2,850.41 cm^{-1} corresponds to C–H stretching of aliphatic $–CH_2$ and $–CH_3$ groups, which are typically found in terpenoids and fatty acids.

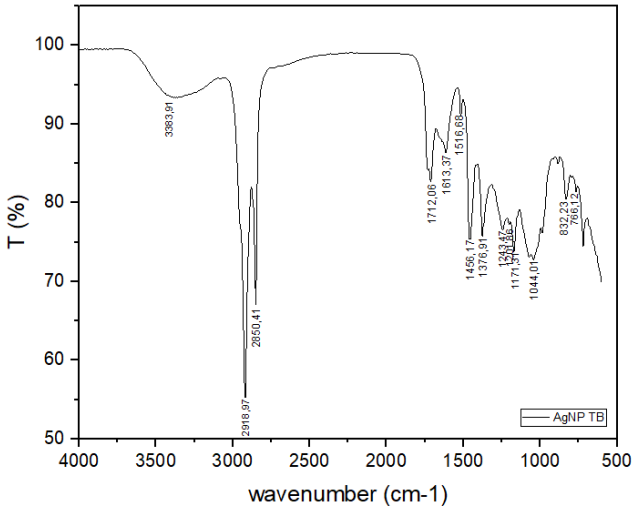

Figure 4: Fourier transmission infra-red (FTIR) of AgNPs biosynthesized using *Ficus deltoidea* leaves extract

The prominent peak at 1,721.96 cm^{-1} is attributable to C=O stretching of carbonyl groups, which may originate from carboxylic acids or ester components. The band at 1,616.86 cm^{-1} is associated with C=C stretching from aromatic rings, suggesting the involvement of flavonoid compounds. The peaks observed at 1,458.37 cm^{-1} and 1,381.51 cm^{-1} correspond to bending vibrations in $–CH_2$ and $–CH_3$ groups, respectively. In the fingerprint region (below 1,300 cm^{-1}), the peaks at 1,249.81 cm^{-1} and 1,140.41 cm^{-1} indicate C–O–C and C–OH stretching vibrations, which are commonly present in flavonoids, glycosides, and polysaccharides. Additionally, the absorptions at 1,033.26 cm^{-1}, 823.21 cm^{-1}, and 617.29 cm^{-1} may be related to C–N stretching (amines), out-of-plane aromatic C–H bending, and metal–oxygen (Ag–O) bond vibrations, respectively. These spectral features confirm that various bioactive compounds from the *F. deltoidea* ethanolic leaf extract played crucial roles in reducing and stabilizing the AgNPs.

The FTIR analysis also revealed the involvement of multiple phytochemicals from *F. deltoidea* in the green synthesis of Fd-AgNPs. The broad O–H stretching vibration at 3,383 cm^{-1} is a strong indicator of polyphenols and flavonoids, which are potent reducing agents.[58,59] These metabolites reduce and stabilize AgNPs by acting as natural reducing and capping agents, where functional groups like hydroxyl (–OH), carboxyl (–COOH), and amine ($–NH_2$) donate electrons for Ag^+ reduction and prevent aggregation.[60] The hydroxyl-rich compounds donate electrons to reduce Ag^+ ions to Ag^0,[61] initiating nanoparticle nucleation. The strong absorption near 1,721.06 cm^{-1} due to C=O stretching is commonly observed in synthesized plant-based AgNPs and is often associated with carboxylic acids or ester groups.[62,63] These carbonyl-containing molecules can act as both reducing and capping agents. Similarly, the C=C aromatic stretching peak at 1,616.86 cm^{-1} supports the hypothesis that flavonoid structures, specifically quercetin and kaempferol derivatives found in *F. deltoidea,* are involved in stabilizing the nanoparticle surface through π–electron interactions.[64,65] Compared with the results of a previous study, which also stated O–H, C=O, and C=C features, the current FTIR spectrum demonstrated a richer fingerprint region, indicating a more diverse phytochemical profile in *F. deltoidea*.[66-68] Furthermore, fewer ether (C–O–C) and amine (C–N) signals and the presence of both glycosidic and amino-based stabilizers potentially enhance nanoparticle stability and bioactivity.[69,70] The peak at 617 cm^{-1} is of particular interest, as it is often linked to metal–oxygen bonding, suggesting the successful formation of Ag–O interactions on the nanoparticle surface. This result is consistent with the findings of Agressott[71], who reported similar low-frequency vibrations in biosynthesized AgNPs, further confirming successful nanoparticle formation.

The XRD pattern of Fd-AgNPs, as shown in Figure 5, revealed distinct diffraction peaks at 2θ values of approximately 27.70°, 32.14°, 38.08°, 44.26°, 46.26°, 54.86°, 57.44°, 64.98°, 67.35°, and 76.36°. Among these, the most intense peaks occurred at 38.08°, 44.26°, 64.98°, and 77.36°, corresponding to the (111), (200), (220), and (311) crystallographic planes of face-centered cubic (fcc) silver, respectively, according to the Joint Committee on Powder Diffraction Standards (JCPDS card no. 04-0783). These reflections confirmed the successful reduction of silver ions (Ag^+) to metallic silver (Ag^0) nanoparticles.

In addition to the major Fd-AgNP peaks, several other diffraction peaks (e.g., at 27.70°, 32.14°, and 46.26°) suggest the presence of additional crystalline phases or organic moieties from *F. deltoidea* bioactive compounds. The broad nature of some peaks, particularly those at approximately 27–35°, may indicate the presence of amorphous organic compounds or phytochemicals capping the nanoparticles. The red arrows in the diffractogram emphasize these secondary peaks, which are most likely due to the crystalline nature of polyphenolic and flavonoid constituents from the plant extract.

The characteristic diffraction peaks at 2θ = 38.08° (111), 44.26° (200), and 64.98° (220) aligned well with earlier studies of biosynthesized AgNPs.[46] The high intensity of the (111) peak suggested that the (111) plane is the most preferentially oriented, which is often associated with increased surface energy and reactivity of the nanoparticles. The presence of additional peaks at approximately 27.70°, 32.14°, and 46.26° is particularly interesting, as it may indicate the influence of plant phytochemicals on the synthesis process. *F. deltoidea* is known to contain flavonoids, tannins, and saponins,[72] which not only act as reducing agents but also function as stabilizers or capping agents. These bioactive compounds can interact with the surface of the AgNPs, creating a bioorganic corona that contributes to the observed secondary diffraction features. For example, phenolic –OH and carboxyl groups in flavonoids can chelate metal ions and promote crystalline or semicrystalline coatings on nanoparticles, potentially explaining the broad and irregular peaks highlighted by red arrows.

Compared with previous reports in which *Azadirachta indica*[73] and *Ocimum sanctum*[74] were used for biosynthesis, the XRD patterns similarly presented characteristic AgNP peaks but lacked some of the minor peaks observed in this study. These findings suggest that *F. deltoidea* may undergo unique structural modifications due to its distinct phytochemical profile. Furthermore, in contrast to the *Moringa oleifera*-mediated synthesis reported by Moodley[41], which demonstrated fewer secondary peaks, the present results indicate greater organic interactions, which may improve the bioactivity or stability of AgNPs for biomedical applications. The interplay of crystalline metallic silver with organic constituents could enhance the antioxidant and antimicrobial capabilities of the nanoparticles. This hybrid structure, revealed through XRD, underscores the potential of *F. deltoidea* as a valuable green synthesis agent for functional nanomaterials.

In Vivo Wound Healing Determination

Table 2 presents the progression of wound healing in mice over 15 days following treatment with different topical ointments, including C−, C+Vas, C+Pov, extract-based ointments (T1–T3), and AgNP-based ointments (T4–T6). On day 0, all the groups had similar wound sizes (0% closure). By day 3, the healing rates of the treatment groups began to diverge. The Fd-AgNP-treated groups, particularly those treated with T6 (30% AgNPs), demonstrated rapid wound healing (46.75 ± 6.75%), significantly outperforming both the extract-only group T3 (18.50 ± 7.35%) and standard treatments such as C+Pov (35.50 ± 6.53%).

On day 6, T4 continued to yield the best effects, with 74.50 ± 4.09% wound closure, followed by T6 (66.25 ± 5.70%) and T2 (60.25 ± 5.79%). Furthermore, on day 9, T4 reached 98.50 ± 0.86%, whereas T6 and T1 reached 95.50 ± 1.65% and 91.75 ± 2.83%, respectively. Notably, complete wound closure (100%) was achieved by day 12 in the mice in the 10% Fd-AgNP-treated groups, whereas the other treatments resulted in full closure only by day 15, except for the C- and C+Vas groups. Although T6 (30% AgNPs) resulted in substantial healing, the 10% Fd-AgNP group (T4) achieved full wound closure earlier (day 12), demonstrating the fastest healing rate among all the groups.

Table 2: Percentage of wound enclosure of mice treated with different topical ointments at several points of day observation

Groups	Wound enclosure percentage at a specific day (%)					
	0	3	6	9	12	15
C-	$_{1}0.00\pm0.00^{a}$	$_{1}9.50\pm5.48^{a}$	$_{2}35.50\pm8.66^{a}$	$_{3}69.50\pm3.17^{a}$	$_{4}93.50\pm1.44^{a}$	$_{5}99.25\pm0.25^{a}$
C+Vas	$_{1}0.00\pm0.00^{a}$	$_{1,2}13.75\pm8.66^{a}$	$_{2,3}38.75\pm9.32^{a}$	$_{3}63.50\pm4.90^{a}$	$_{4}91.75\pm2.83^{a}$	$_{5}99.50\pm0.28^{ab}$
C+Pov	$_{1}0.00\pm0.00^{a}$	$_{2}35.50\pm6.53^{bc}$	$_{3}63.50\pm4.90^{bc}$	$_{4}89.50\pm4.97^{cd}$	$_{5}99.75\pm0.25^{bc}$	$_{5}100.00\pm0.00^{b}$
T1	$_{1}0.00\pm0.00^{a}$	$_{2}18.50\pm7.35^{ab}$	$_{3}50.50\pm5.72^{ab}$	$_{4}91.75\pm2.83^{cd}$	$_{5}98.75\pm0.94^{bc}$	$_{5}100.00\pm0.00^{b}$
T2	$_{1}0.00\pm0.00^{a}$	$_{2}35.50\pm6.53^{bc}$	$_{3}60.25\pm5.79^{bc}$	$_{4}85.25\pm3.79^{bc}$	$_{5}98.50\pm0.86^{b}$	$_{5}100.00\pm0.00^{b}$
T3	$_{1}0.00\pm0.00^{a}$	$_{2}18.50\pm7.35^{ab}$	$_{3}46.75\pm6.75^{ab}$	$_{4}86.50\pm4.55^{bcd}$	$_{4,5}97.50\pm2.17^{abc}$	$_{5}100.00\pm0.00^{b}$
T4	$_{1}0.00\pm0.00^{a}$	$_{2}46.75\pm6.75^{c}$	$_{3}74.50\pm4.09^{c}$	$_{4}98.50\pm0.86^{e}$	$_{5}100.00\pm0.00^{c}$	$_{5}100.00\pm0.00^{b}$
T5	$_{1}0.00\pm0.00^{a}$	$_{2}35.50\pm6.53^{bc}$	$_{2,3}56.50\pm8.41^{abc}$	$_{3}76.25\pm5.58^{ab}$	$_{4}98.00\pm1.15^{abc}$	$_{5}100.00\pm0.00^{b}$
T6	$_{1}0.00\pm0.00^{a}$	$_{2}46.75\pm6.75^{c}$	$_{2}66.25\pm5.70^{bc}$	$_{3}95.50\pm1.65^{de}$	$_{4}99.75\pm0.25^{bc}$	$_{5}100.00\pm0.00^{b}$

Note: C-: without treatment; C+Vas: vaseline; C+Pov: *povidone iodine*; T1-T3: with 10; 20; 30 % of extract ointment; T4-T6: with 10; 20; 30 % of AgNPs synthesized using *Ficus deltoidea*. Mean ± SE followed by different *superscript* letters (a, b, c, d, e) at the same column and *subscript* number (1, 2, 3, 4, 5) at the same row, indicated significantly different ($p<0.05$).

The nanoscale size of AgNPs increases their surface area and improves their bioavailability, facilitating deeper penetration into the wounded tissue.[17,75] A similar previous study revealed that green-synthesized AgNPs from *Moringa oleifera* accelerate epithelial healing faster than plant extracts.[76,77] Additionally, polyphenol-capped AgNPs exhibited superior antimicrobial and pro-healing activity because of their ability to modulate oxidative stress and increase the fibroblast number.[21,78,79] This finding aligns with the current study, where Fd-AgNPs rich in polyphenolic compounds showed potent healing effects in T4. Therefore, T4 (10% Fd-AgNPs) emerged as the most promising formulation in this study, offering a biocompatible, efficient, and rapid wound-healing agent. Its efficacy supports the further development of green-synthesized AgNPs as topical therapeutics for clinical wound management. In addition, the comparative results clearly indicated that compared with the other groups, the T4–T6 (Fd-AgNPs) topical ointments are better for promoting wound healing. This is evidenced by the high fibroblast count and complete wound closure observed, aligning with the crucial phases of wound healing: inflammation, proliferation, and remodeling.

The biochemical and cellular markers related to wound healing, protein content, hydroxyproline level, total DNA content, and fibroblast count

from mouse wound tissues treated with various topical ointments are summarized in Table 3. While T6 effectively promoted wound healing, the 20% AgNP group (T5) presented increased protein, hydroxyproline, and DNA levels and increased fibroblast counts, indicating a more robust regenerative response overall. The protein content in the T6 group was 600.87 ± 34.90 was lower than that in the C− (1,323.37 ± 59.76) and C+Vas (1,306.81 ± 54.33) groups but significantly greater ($p < 0.05$) than that in the T4 (10% AgNP) and 20% extract (T2) groups. However, T5 (20% AgNPs) had the highest protein content among the treated groups (961.81 ± 90.67), indicating robust tissue regeneration. The presence of high fibroblast numbers in T5-treated wounds is especially critical, as fibroblasts produce extracellular matrix components, including collagen and elastin, facilitating the dermal integrity and tensile strength of healed skin[80,81].

Table 3: Mean of Protein content, Hydroxyproline level, and Total DNA of wound tissue of mice treated with different topical ointment

Groups	Protein content (µg/mL)	Hydroxyproline level (µg/mL)	Total DNA (µg/mL)	Number of Fibroblast
C-	1323.37±59.76^{d}	4210.25±44.65^{f}	6.29±0.40^{c}	1.87±0.00^{c}
C+Vas	1306.81±54.33^{d}	4206.50±44.86^{f}	6.28±0.29^{c}	1.79±0.07^{bc}
C+Pov	649.00±69.17^{ab}	3453.16±56.47^{cd}	3.59±0.33^{ab}	1.72±0.08^{abc}
T1	602.43±65.16^{ab}	3380.66±48.50^{bc}	3.47±0.23^{ab}	1.65±0.07^{ab}
T2	784.62±124.26^{bc}	3606.08±78.30^{de}	3.70±0.31^{ab}	1.72±0.08^{abc}
T3	717.7±105.93^{b}	3558.16±57.62^{cde}	3.67±0.26^{ab}	1.79±0.07^{bc}
T4	452.75±44.40^{a}	3146.50±79.54^{a}	2.89±0.10^{a}	1.58±0.00^{a}
T5	961.81±90.67^{c}	3732.33±46.59^{e}	4.10±0.15^{b}	1.79±0.07^{bc}
T6	600.87±34.09^{ab}	3247.75±67.89^{ab}	3.07±0.09^{a}	1.72±0.08^{abc}

Note: C-: without treatment; C+Vas: vaseline; C+Pov: *povidone iodine*; T1-T3: with topical ointment containing 10; 20; 30 % of *Ficus deltoidea* extract; T4-T6: with topical ointment containing 10; 20; 30 % of AgNPs synthesized using *Ficus deltoidea*. Mean ± SE followed by different *superscript* letters (a-e) at the same column, indicated significant differences ($p<0.05$).

Regarding hydroxyproline levels, which reflect the collagen content, T5 again presented the highest value among the treated groups (3,732.35 ± 344.96), followed by T2 and T3. Although T6 (3,247.75 ± 67.98) had a slightly lower hydroxyproline level, it was still significantly greater than that of T4, indicating effective collagen deposition. The total DNA content, a proxy for cellular proliferation, was highest in T5 (4.10 ± 0.15), followed closely by T2 and T3. The T6 group maintained a relatively high value (3.07 ± 0.09), which was not significantly different ($p > 0.05$) from those of the other effective groups.

Most notably, the number of fibroblasts, which are key cells in wound healing, was highest in the C– group (1.87 ± 0.00), which was equal to the number of fibroblasts in both the 30% *F. deltoidea* ethanolic leaf extract-treated and the Fd-AgNP-treated (T3 and T5) wound groups. Despite a moderate fibroblast number, T6 showed rapid wound closure, suggesting that its performance may be more related to antimicrobial or anti-inflammatory properties than to its ability to proliferate alone.

Further, the higher protein content, hydroxyproline levels, and total DNA observed in the C− (untreated) and C+Vas (Vaseline-treated) groups are likely due to delayed wound healing, resulting in prolonged fibroblast activity and extracellular matrix synthesis. In contrast, the C+Pov (povidone-iodine) and Fd-AgNP-treated groups (T4–T6) exhibited faster wound closure, leading to reduced levels of these biomarkers by day 10, as tissue regeneration was already more advanced. This indicates that while C− and C+Vas had ongoing tissue repair processes, the treated groups had transitioned to later healing phases with less cellular proliferation.

The enhanced performance of AgNP-treated wounds can be mechanistically linked to the bioactive compounds identified in the FTIR spectrum (Figure 4), where peaks at 3,393.91 cm^{-1} (O–H), 1,721.96 cm^{-1} (C=O), and 1,616.86 cm^{-1} (C–C) confirmed the presence of phenolic groups, flavonoids, and amide bonds. These functional groups are responsible for reducing Ag^{+} ions to form and stabilize nanoparticles. Moreover, these biomolecules possess antioxidant, anti-inflammatory, and antimicrobial activities, directly contributing to improved healing efficiency.[82-84]

Compared with extract-only treatments (T1–T3), AgNPs delivered superior performance. Extract-only ointments had moderate effects on protein and hydroxyproline contents but lacked the cellular response needed for complete closure. These findings suggest that AgNPs enhance bioavailability and facilitate the sustained release of phytochemicals, improving penetration into the wound bed and ensuring prolonged therapeutic action. These findings are consistent with a recent study demonstrating that polyphenol-loaded AgNPs accelerated fibroblast activity and improved wound tensile strength.[85,86] Similarly, AgNPs synthesized from *Moringa oleifera* also enhanced wound healing through increased collagen and fibroblast presence.[87]

Furthermore, T4 and T6 formulations demonstrated the fastest wound closure; the lower protein content, hydroxyproline level, and fibroblast number suggest that wound contraction occurred rapidly but possibly without the full depth of tissue remodeling seen in other groups. T5 (20% Fd-AgNPs), however, exhibited slightly slower but still efficient wound closure, coupled with the highest levels of total protein, hydroxyproline, and DNA and a greater fibroblast count. These indicators reflect robust extracellular matrix synthesis and active cellular proliferation, which are essential for long-term structural integrity and functional recovery of the skin. Therefore, while T4 and T6 may be optimal for rapid re-epithelialization, T5 appears superior in promoting complete and biologically rich tissue regeneration. This finding suggests that T5 may provide a better balance between healing speed and quality, making it the most promising formulation for achieving both rapid and structurally sound wound healing.

Histological observations of wound tissues collected from mice after 10 days of treatment with various topical ointments revealed distinct differences in fibroblast proliferation and tissue regeneration among the groups (Figure 6). In the C– group, minimal fibroblast activity was visible, with few fibroblasts (indicated by arrows) and incomplete epidermal regeneration. Similarly, the C+Vas and C+Pov groups presented moderate fibroblast presence and slightly improved tissue architecture but still presented incomplete epithelial continuity.

In contrast, groups T1–T3 presented increased fibroblast numbers, especially at the 20% concentration (T2), where the fibroblast density increased noticeably, and the dermal layer appeared more organized.

ISSN 2616-0684 (Print)
ISSN 2616-0692 (Electronic)

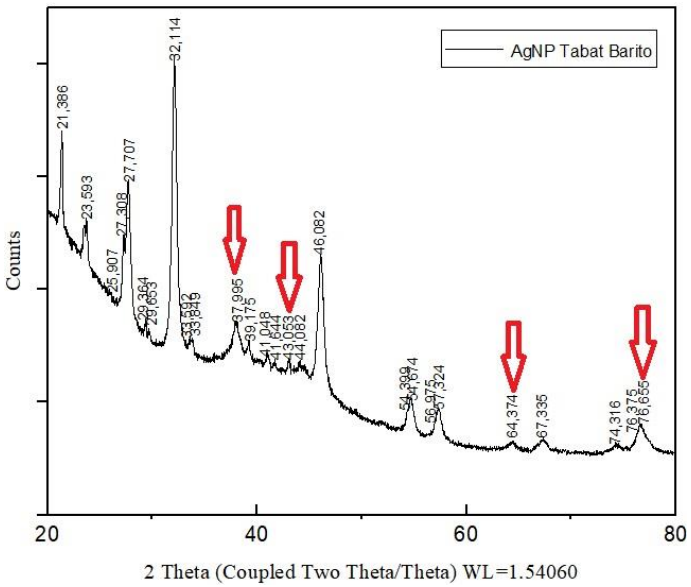

Figure 5: X-Ray diffractogram of AgNPs biosynthesized using *Ficus deltoidea* leaves extract

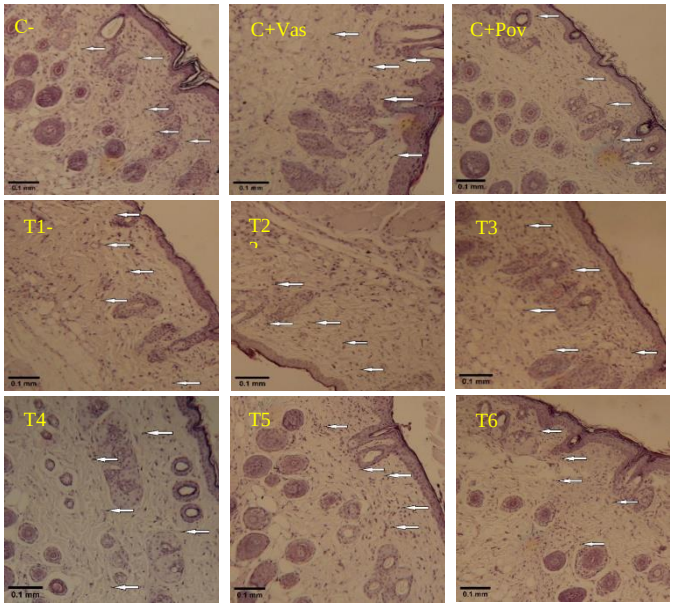

Figure 6: Histology determination of wound tissue of mice after 10 days treated with different topical ointment. Note**:** C-: without treatment; C+Vas: vaseline; C+Pov: *povidone iodine*; T1-T3: with topical ointment containing 10; 20; 30 % of *Ficus deltoidea* extract; T4-T6: with topical ointment containing 10; 20; 30 % of AgNPs synthesized using *Ficus deltoidea* ethanol eaf extract; white arrows→fibroblast.

The most significant histological improvement was observed in groups T4–T6. Among these groups, most treatments (extract and AgNPs) presented a high density of fibroblasts (except T4), marked by numerous spindle-shaped fibroblastic cells throughout the dermis. Moreover, complete re-epithelialization and organized tissue layers were apparent, suggesting advanced stages of wound remodeling.

The histological findings corroborate the biochemical and morphological data from previous analyses (protein content, hydroxyproline, SEM, FTIR, and XRD). The increased fibroblast number and well-structured tissue regeneration observed, particularly in the T6 group, suggest the superior wound healing performance of the Fd-AgNPs. This enhanced effect is attributed to the intrinsic properties of the AgNPs and the bioactive phytochemicals from the plant extract that capped and stabilized the nanoparticles. The observed number of fibroblasts aligns with the data from Table 2, where all groups, except T4, presented high fibroblast counts. Fibroblasts are essential for collagen deposition, extracellular matrix formation, and overall wound closure, and their abundance indicates efficient tissue remodeling. These findings suggest that the synergistic action of AgNPs and *F. deltoidea* compounds accelerates wound healing by promoting fibroblast activity. Comparable results have been reported in a previous study by Galdopórpora[88], where polyphenol-coated silver nanoparticles improved fibroblast migration and collagen synthesis in tissue engineering. Thus, the histological evidence from the present study strongly supports the therapeutic potential of Fd-AgNPs, particularly at a 30% concentration (T6). T6 supported effective tissue regeneration; however, the T4 and T5 formulations also demonstrated key advantages in terms of healing speed and cellular activity, respectively. While T6 (30% Fd-AgNPs) resulted in rapid wound closure, T4 (10%) achieved complete closure earlier (day 12), and both T4 and T6 had similar healing rates, with no significant differences by days 9 and 12. This indicates that increasing the concentration of Fd-AgNPs does not linearly enhance wound-healing efficacy. Therefore, the results suggest an optimal concentration range rather than a dose-dependent response, with T4 and T5 offering the best balance between speed and quality of tissue regeneration.

The Fd-AgNPs enhance metabolite penetration into the wound bed due to their small size and high surface area, allowing deeper tissue access. The Fd-AgNPs also act as carriers for bioactive compounds, enabling sustained and localized release at the wound site. Additionally, AgNPs reduce inflammation and microbial load, creating a favorable environment for better absorption and tissue regeneration.

Conclusion

The study demonstrated that green-synthesized Fd-AgNPs significantly enhanced wound healing compared to the controls. Among all formulations, 10% Fd-AgNP (T4) achieved complete wound closure by day 12, while 20% Fd-AgNP (T5) showed the highest protein, hydroxyproline, DNA content, and fibroblast count, indicating stronger regenerative activity. Although 30% Fd-AgNP (T6) also showed rapid closure, no dose-dependent effect was observed. Mice treated with T5 demonstrated the best balance between healing speed and tissue quality. Histological findings further confirmed improved fibroblast activity and tissue organization in Fd-AgNP-treated groups. These results suggest that 20% Fd-AgNP is the most effective formulation for achieving rapid and structurally robust wound healing, supporting its potential as a natural, biocompatible topical therapy.

Conflict of Interest

The authors declare no conflict of interest.

Authors' Declaration

The authors hereby declare that the work presented in this article are original and that any liability for claims relating to the content of this article will be borne by them.

Acknowledgments

The authors express their sincere gratitude to the Faculty of Mathematics and Natural Sciences, Mulawarman University, for providing laboratory facilities and research support throughout the study. Special thanks are extended to the technical staff of the Animal Anatomy and Microtechnique Laboratory, as well as the Animal Physiology, Development, and Molecular Laboratory, for their valuable assistance during the experimental phases. The authors also appreciate the postgraduate program for supporting research collaboration and knowledge sharing during this project.

References

1. Abdulrahman MD. Crude extract of *Ficus deltoidea* Jack (FD) as a natural biological therapy. Explor target anti-tumor ther. 2023; 4(1):57–88.
2. Raihandhany R, Zen TV. Exploring the less prominent relatives of *Ficus benjamina* L. in Indonesia A review on the botanical, ethnobotanical, and future perspectives of *Ficus deltoidea* Jack. and *Ficus septica* Burm. f. Genbinesia J Biol. 2022; 1(2):76-89.
3. Abrahim NN, Abdul-Rahman PS, Aminudin N. The antioxidant activities, cytotoxic properties, and identification of water-soluble compounds of *Ficus deltoidea* leaves. PeerJ. 2018; 6:1-20.
4. Ashraf K, Haque MR, Amir M, Ahmad N, Ahmad W, Sultan S, Shah SAA, Alafeefy AM, Mujeeb M, Shafie MFB. An Overview of Phytochemical and Biological Activities: *Ficus deltoidea*: Jack and Other: *Ficus*: spp. J Pharm Bioallied Sci. 2021; 13(1):11-25.
5. Aryani R, Nugroho RA, Manurung H, Mardayanti R, Prahastika W, Karo APB. *Ficus deltoidea* leaves methanol extract promote wound healing activity in mice. EurAsian J BioSci. 2020; 14(1):85-91.
6. Lakkim V, Reddy MC, Lekkala VV, Lebaka VR, Korivi M, Lomada D. Antioxidant efficacy of green-synthesized silver nanoparticles promotes wound healing in mice. Pharmaceutics. 2023; 15(5):1517.
7. Mamun AA, Shao C, Geng P, Wang S, Xiao J. Recent advances in molecular mechanisms of skin wound healing and its treatments. Front Immunol. 2024; 15(1):1-29.
8. Venkatesan K, Sivadasan D, Abderrahmen Al Weslati M, Gayasuddin Mouid M, Goyal M, Bansal M, Salama ME-DM, Azizullah Ghori S, Ahmad F. Protective Effects of Frankincense Oil on Wound Healing: Downregulating Caspase-3 Expression to Facilitate the Transition from the Inflammatory to Proliferative Phase. Pharmaceuticals. 2025; 18(3):407.
9. Cioce A, Cavani A, Cattani C, Scopelliti F. Role of the skin immune system in wound healing. Cells. 2024; 13(7):624.
10. Suhag D. Skin and Wound Healing Biomaterials. Handbook of Biomaterials for Medical Applications, Volume 2: Applications: Springer; 2024. p. 281-320.
11. Uberoi A, McCready-Vangi A, Grice EA. The wound microbiota: microbial mechanisms of impaired wound healing and infection. Nat Rev Microbiol. 2024; 22(8):507-521.
12. Kumar P, Hasan F, Kumar V, Chawla R, Goyal SK. Diabetic Wound Healing: Navigating Physiology, Advancements and Research Frontiers. J Diabetes Res. 2024; 6(2):1-11.
13. Pramasari N, Anjani AG, Muslikh FA, Lestari TP, Shoviantari F, Septyaningrum SD, Melati IS, Randy GY. Green Synthesis, Optimization and Characterization of Carrot Extract Silver Nanoparticles. Trop J Pharm Res. 2024; 8(12):1-5.
14. Alavi SE, Alavi SZ, Nisa MU, Koohi M, Raza A, Ebrahimi Shahmabadi H. Revolutionizing wound healing: exploring scarless solutions through drug delivery innovations. Mol Pharm. 2024; 21(3):1056-1076.
15. Banerjee D, Vydiam K, Vangala V, Mukherjee S. Advancement of Nanomaterials-and Biomaterials-Based Technologies for Wound Healing and Tissue Regenerative Applications. ACS Appl Bio Mater. 2025; 8(3):1877–1899.
16. Ullah A, Ullah M, Lee G-J, Lim SI. A review of recent advances in nanotechnology for the delivery of therapeutics in wound healing. J Pharm Investig. 2025; 55(1):33-54.
17. Jangid H, Singh S, Kashyap P, Singh A, Kumar G. Advancing biomedical applications: An in-depth analysis of silver nanoparticles in antimicrobial, anticancer, and wound healing roles. Front Pharmacol. 2024; 15(1):1-26.
18. Nqakala ZB, Sibuyi NR, Fadaka AO, Meyer M, Onani MO, Madiehe AM. Advances in nanotechnology towards development of silver nanoparticle-based wound-healing agents. Int J Mol Sci. 2021; 22(20):1-26.
19. Naganthran A, Verasoundarapandian G, Khalid FE, Masarudin MJ, Zulkharnain A, Nawawi NM, Karim M, Che Abdullah CA, Ahmad SA. Synthesis, characterization and biomedical application of silver nanoparticles. Materials. 2022; 15(2):427.
20. Ranjbar S, Bakhtiari A, Khosravi N, Ashkavandi SJ, Azamian F, Alijaniha M, Karbalaee M. Silver nanoparticles: Biomedical applications and future perspectives. JCC. 2024; 6(20):1-13.
21. Ren Y, Zhang Y, Li X. Application of AgNPs in biomedicine: An overview and current trends. Nanotechnol Rev. 2024; 13(1):1-17.
22. More PR, Pandit S, Filippis AD, Franci G, Mijakovic I, Galdiero M. Silver nanoparticles: bactericidal and mechanistic approach against drug resistant pathogens. Microorganisms. 2023; 11(2):369-396.
23. Tripathi N, Goshisht MK. Recent advances and mechanistic insights into antibacterial activity, antibiofilm activity, and cytotoxicity of silver nanoparticles. ACS Appl Bio Mater. 2022; 5(4):1391-1463.
24. Fu W, Sun S, Cheng Y, Ma J, Hu Y, Yang Z, Yao H, Zhang Z. Opportunities and challenges of nanomaterials in wound healing: Advances, mechanisms, and perspectives. Chem Eng J. 2024:153640.
25. Nandhini J, Karthikeyan E, Rani EE, Karthikha V, Sanjana DS, Jeevitha H, Rajeshkumar S, Venugopal V, Priyadharshan A. Advancing engineered approaches for sustainable wound regeneration and repair: Harnessing the potential of green synthesized silver nanoparticles. Eng Regen. 2024; 5(3):306-325.
26. Sati A, Ranade TN, Mali SN, Ahmad Yasin HK, Pratap A. Silver Nanoparticles (AgNPs): Comprehensive Insights into Bio/Synthesis, Key Influencing Factors, Multifaceted Applications, and Toxicity─ A 2024 Update. ACS omega. 2025; 10(8):7549-7582.
27. Shahzadi S, Fatima S, Shafiq Z, Janjua MRSA. A review on green synthesis of silver nanoparticles (SNPs) using plant extracts: a multifaceted approach in photocatalysis, environmental remediation, and biomedicine. RSC Adv. 2025; 15(5):3858-3903.
28. Dhir R, Chauhan S, Subham P, Kumar S, Sharma P, Shidiki A, Kumar G. Plant-mediated synthesis of silver nanoparticles: unlocking their pharmacological potential–a comprehensive review. Front bioeng biotechnol. 2024; 11:1324805.
29. Kar AK, Singh A, Singh D, Shraogi N, Verma R, Saji J, Jagdale P, Ghosh D, Patnaik S. Biopolymeric composite hydrogel loaded with silver NPs and epigallocatechin gallate (EGCG) effectively manages ROS for rapid wound healing in type II diabetic wounds. Int J Biol Macromol. 2022; 218:506-518.
30. Ahmad A, Haneef M, Ahmad N, Kamal A, Jaswani S, Khan F. Biological synthesis of silver nanoparticles and their medical applications. World Acad Sci J. 2024; 6(3):22.
31. Yi Q, Huang Z, Tang B. Impact of Silver Dressings on Wound Healing Rate in Patients with Lower Extremity Ulcers: A Systematic Review and Meta-Analysis of Randomized Controlled Trials. Med Princ Pract. 2025; 34(1):13-24.
32. Jain K, Takuli A, Gupta TK, Gupta D. Rethinking nanoparticle synthesis: a sustainable approach vs. traditional methods. Chem Asian J. 2024; 19(21):e202400701.
33. Aryani R, Nugroho RA, Manurung H, Rulimada MH, Maytari E, Siahaan A, Rudianto R, Jati WN. Anti-angiogenic activity of *Ficus deltoidea* L. Jack silver nanoparticles using chorioallantoic membrane assay. F1000Res. 2023; 12(1):544-560.
34. Antunes Filho S, Almeida CM, Romanos MTV, Pizzorno Backx B, Regina Bonelli R. Green synthesis of silver nanoparticles for functional cotton fabrics: antimicrobial efficacy against multidrug-resistant bacteria and cytotoxicity evaluation. Artif Cells Nanomed Biotechnol. 2025; 53(1):153-165.
35. Das R, Kumar P, Singh AK, Agrawal S, Albukhaty S, Bhattacharya I, Tiwari KN, Mishra SK, Tripathi AK, AlMalki FA. Green synthesis of silver nanoparticles using *Trema*

orientalis (L.) extract and evaluation of their antibacterial activity. Green Chem Lett Rev. 2025; 18(1):1-14.
36. Karimi M, Parsaei P, Asadi SY, Ezzati S, Boroujeni RK, Zamiri A, Rafieian-Kopaei M. Effects of *Camellia sinensis* ethanolic extract on histometric and histopathological healing process of burn wound in rat. 2013; 13(1):14-19.
37. Hada A-M, Suarasan S, Muntean M, Potara M, Astilean S. Aptamer-conjugated gold nanoparticles for portable, ultrasensitive naked-eye detection of C-reactive protein based on the Tyndall effect. Anal Chim Acta. 2024; 1307:342626-342637.
38. Yuan K, Sun Y, Liang F, Pan F, Hu M, Hua F, Yuan Y, Nie J, Zhang Y. Tyndall-effect-based colorimetric assay with colloidal silver nanoparticles for quantitative point-of-care detection of creatinine using a laser pointer pen and a smartphone. RSC Adv. 2022; 12(36):23379-23386.
39. Barzinjy AA, Haji BS. Green synthesis and characterization of Ag nanoparticles using fresh and dry *Portulaca oleracea* leaf extracts: Enhancing light reflectivity properties of ITO glass. Micro nano lett. 2024; 19(3):1-13.
40. Ezeh CK, Eze CN, Dibua MUE, Emencheta SC. A review on *Azadirachta indica* (neem) plant mediated biosynthesis, characterisation and antimicrobial activity of silver nanoparticles. IJBNN. 2024; 5(1):15-36.
41. Moodley JS, Krishna SBN, Pillay K, Sershen f, Govender P. Green synthesis of silver nanoparticles from *Moringa oleifera* leaf extracts and its antimicrobial potential. Adv Nat Sci Nanosci Nanotechnol. 2018; 9(1):015011.
42. Bunawan H, Amin NM, Bunawan SN, Baharum SN, Mohd Noor N. *Ficus deltoidea* Jack: a review on its phytochemical and pharmacological importance. Evid Based Complement Alternat Med. 2014; 2014(1):902734.
43. Habeeb Rahuman HB, Dhandapani R, Narayanan S, Palanivel V, Paramasivam R, Subbarayalu R, Thangavelu S, Muthupandian S. Medicinal plants mediated the green synthesis of silver nanoparticles and their biomedical applications. IET nanobiotechnol. 2022; 16(4):115-144.
44. Kirubakaran D, Wahid JBA, Karmegam N, Jeevika R, Sellapillai L, Rajkumar M, SenthilKumar KJ. A Comprehensive Review on the Green Synthesis of Nanoparticles: Advancements in Biomedical and Environmental Applications. Biomed Mater Devices. 2025; 1(1):1-13.
45. Chandrasekaran M, Chinnaiyan U, Sivaprakasam S. Biogenic Synthesis and Characterization of Silver Nanoparticles Using a Combined Leaf Extract for Anti-Bacterial and Biofilm Inhibition Properties. Trop J Pharm Res. 2025; 9(3):1089-1096.
46. Vanlalveni C, Lallianrawna S, Biswas A, Selvaraj M, Changmai B, Rokhum SL. Correction: green synthesis of silver nanoparticles using plant extracts and their antimicrobial activities: a review of recent literature. RSC Adv. 2022; 12(25):16093-16093.
47. Kantoma D, Nwokem CO. Green Synthesis of Silver Nanoparticles (AgNPs) using *Calotropis procera* Leaves Extract and it Adsorption Properties for the Removal of Cr^{3+} from Petroleum Waste Water. Comm Phy Sci. 2023; 10(3):214-223.
48. Abdel-Rahman LH, Al-Farhan BS, Abou El-ezz D, Abd–El Sayed MA, Zikry MM, Abu-Dief AM. Green Biogenic Synthesis of Silver Nanoparticles Using Aqueous Extract of *Moringa oleifera*: Access to a Powerful Antimicrobial, Anticancer, Pesticidal and Catalytic Agents. J Inorg Organomet Polym Mater. 2022; 32(4):1422-1435.
49. Kaur R, Avti P, Kumar V, Kumar R. Effect of various synthesis parameters on the stability of size controlled green synthesis of silver nanoparticles. Nano Express. 2021; 2(2):020005-020019.
50. Alam A, Mazumder PM. The Application of Ficus Species in the Treatment of Neurological Disorders. Pharmacogn Mag. 2024; 21(2):323–335.
51. Gunti H, Gaddam SA, Nadipi R, Kotakadi VS. Optical and Paper-based Dual Sensing of Hg^{2+} and Colorimetric Reduction of Cr (VI) by Green Synthesized Silver Nanoparticles Prepared from the Bark Extract of *Sweetinia mahagoni* and Their Promising Antimicrobial Applications. Nano Biomed Eng. 2023; 15(1):60-73.
52. Nagaraja SK, Niazi SK, Bepari A, Assiri RA, Nayaka S. *Leonotis nepetifolia* flower bud extract mediated green synthesis of silver nanoparticles, their characterization, and in vitro evaluation of biological applications. Materials. 2022; 15(24):8990-9010.
53. Dubey N, Dubey N. Current regulatory framework in nanotechnology and medicine. Nanotechnology in Medicine: Toxicity and Safety. 2021:373-406.
54. Labuda J, Barek J, Gajdosechova Z, Goenaga-Infante H, Johnston LJ, Mester Z, Shtykov S. Analytical chemistry of engineered nanomaterials: Part 1. Scope, regulation, legislation, and metrology (IUPAC Technical Report). PAC. 2023; 95(2):133-163.
55. Din SM, Malek NANN, Shamsuddin M, Matmin J, Hadi AA, Asraf MH. Antibacterial silver nanoparticles using different organs of *Ficus deltoidea* Jack var. kunstleri (King) Corner. Biocatal Agric Biotechno. 2022; 44:102473.
56. Ismail IQ, Malek NANN, Sani NS, Din SM, Asraf MH. Green Biosynthesized Silver Nanoparticles using *Ficus deltoidea* Leaf Extract as Antibacterial Agent. Bioresour Enviro. 2023; 1(3):27-44.
57. Sharma K, Guleria S, Razdan VK. Green synthesis of silver nanoparticles using *Ocimum gratissimum* leaf extract: characterization, antimicrobial activity and toxicity analysis. J Plant Biochem Biotechnol. 2020; 29(2):213-224.
58. Mamouni R, Jadouali S, Atifi H, Saffaj N, Chartier A, Nehme R, Boussif K, Achemchem F. A novel green reducing agent for the synthesis of chromium oxide nanoparticles (Cr_2O_3 NPs) based on saffron by-products: Characterization and antioxidant activity. Mater Sci Eng B. 2024; 305:117415.
59. Terenteva E, Apyari V, Dmitrienko S, Zolotov YA. Formation of plasmonic silver nanoparticles by flavonoid reduction: A comparative study and application for determination of these substances. SAA. 2015; 151:89-95.
60. Godeto YG, Ayele A, Ahmed IN, Husen A, Bachheti RK. Medicinal plant-based metabolites in nanoparticles synthesis and their cutting-edge applications: an overview. 2023; 1(1):1-34.
61. Khan MR, Ahmad K, Akram R, Asif HM, Ahmad B, Ali T, Anjum I, Sami A, Bibi A, Saifullah S. Green synthesis, characterization and antibacterial potential of silver nanoparticles from Onosma bracteatum extract. Trop J Pharm Res. 2022; 6(2):202-206.
62. Alharbi NS, Alsubhi NS. Silver Nanoparticles Biosynthesized Using *Azadirachta indica* Fruit and Leaf Extracts: Optimization, Characterization, and Anticancer Activity. J Nanomater. 2023; 2023(1):1-17.
63. Lan-Chi NT, Narayanan M, Chinnathambi A, Govindasamy C, Subramani B, Brindhadevi K, Pimpimon T, Pikulkaew S. Fabrication, characterization, anti-inflammatory, and anti-diabetic activity of silver nanoparticles synthesized from *Azadirachta indica* kernel aqueous extract. Environ Res. 2022; 208:112684.
64. Liu L, Yu C, Ahmad S, Ri C, Tang J. Preferential role of distinct phytochemicals in biosynthesis and antibacterial activity of silver nanoparticles. J Environ Manage. 2023; 344:118546.
65. Reddy K, Salve P. Biogenic synthesis of silver nanoparticles from *Hylocereus undatus* peel waste: exploring EGFR inhibition for targeted therapy of cervical and breast carcinomas. Futur J Pharm Sci. 2024; 10(1):160.
66. Elish SEAA, Temraz A, Hassan Baky M. Phytochemical diversity of genus Ficus: A mini review. ERU Res J. 2023; 2(3):502-524.
67. Ikhsan AN, Syifa F, Mustafidah M, Rohman A. Implementation of chemometrics as a Solution to detecting and preventing

falsification of herbal medicines in Southeast Asia: A review. J Appl Pharm Sci. 2021; 11(9):139-148.
68. Samsulrizal N, Yong-Meng G, Ahmad H, Syimal'ain Azmi N, Mohamad Zin NSN, Mahdi E. Infrared spectral markers for the nephroprotective effects of *Ficus deltoidea* in streptozotocin-induced diabetic rats. BioRxiv. 2020; 1(1):1-37.
69. Sidhu AK, Verma N, Kaushal P. Role of biogenic capping agents in the synthesis of metallic nanoparticles and evaluation of their therapeutic potential. Front Nanotechnol. 2022; 3:801620-801637.
70. Zhu W, Wu J, Guo X, Sun X, Li Q, Wang J, Chen L. Development and physicochemical characterization of chitosan hydrochloride/sulfobutyl ether-β-cyclodextrin nanoparticles for cinnamaldehyde entrapment. J Food Biochem. 2020; 44(6):e13197.
71. Agressott EVH, Blätte D, Cunha FA, Noronha VT, Ciesielski R, Hartschuh A, Paula AJ, Fechine PBA, Souza Filho AG, Paschoal AR. Vibrational Spectroscopy and Morphological Studies on Protein-Capped Biosynthesized Silver Nanoparticles. ACS omega. 2020; 5(1):386-393.
72. Santhanam R, Sivapragasam G, Karunakaran T, Muniandy K, Kandasamy SP, Palanisamy A. Identification of chemical constituents and inhibitory effect of *Ficus deltoidea* fraction against lipopolysaccharide-induced nuclear factor-kappa B inflammatory pathway in murine macrophage 264.7 cells. harmacogn Mag. 2021; 17(74):236-243.
73. Renuka R, Thilagavathi T, Inmozhi C, Uthrakumar R, Rajasaravanan ME, Kaviyarasu K, Al-Taisan NA, Awad M, Alam MW. Phytochemical Investigation and Characterization of Azadirachta Indica-Mediated Silver Nanoparticles and Their Potential as Antibacterial and Antidiabetic Agents. 2024; 19(10):2450061.
74. Sulaiman M, Muhammad MaA, Sulaiman AS, Abubakar AL, Sharma R, Shuaibu AM, Aliyu M, Mustapha ITu, Tiwari R. Antimicrobial Potential and Characterization of Silver Nanoparticles Synthesized from *Ocimum sanctum* Extract. 2024; 1(1):1-16.
75. Bold BE, Urnukhsaikhan E, Mishig-Ochir T. Biosynthesis of silver nanoparticles with antibacterial, antioxidant, anti-inflammatory properties and their burn wound healing efficacy. Front chem. 2022; 10:972534.
76. Islam A, Mandal C, Habib A. Antibacterial potential of synthesized silver nanoparticles from leaf extract of *Moringa oleifera*. J Adv Biotechnol Exp Ther. 2021 2021; 4(1):67.
77. Mehwish HM, Liu G, Rajoka MSR, Cai H, Zhong J, Song X, Xia L, Wang M, Aadil RM, Inam-Ur-Raheem M, Xiong Y, Wu H, Amirzada MI, Zhu Q, He Z. Therapeutic potential of *Moringa oleifera* seed polysaccharide embedded silver nanoparticles in wound healing. Int J Biol Macromol. 2021; 184:144-158.
78. Adeyemi OS, Shittu EO, Akpor OB, Rotimi D, Batiha GE-s. Silver nanoparticles restrict microbial growth by promoting oxidative stress and DNA damage. EXCLI J. 2020; 19:492.
79. Rodrigues AS, Batista JG, Rodrigues MÁ, Thipe VC, Minarini LA, Lopes PS, Lugão AB. Advances in silver nanoparticles: a comprehensive review on their potential as antimicrobial agents and their mechanisms of action elucidated by proteomics. Front Microbiol. 2024; 15:1440065.
80. Aguilera Stewart C, Alar C, Bargsted L, Kaklamanou I, Gozza GA, Polito MP, Enzo E, Sifrim A, Aragona M. Defining the role of fibroblasts in skin expansion. BioRxiv. 2025; 1(1):2025-2078.
81. Dong X, Xiang H, Li J, Hao A, Wang H, Gou Y, Li A, Rahaman S, Qiu Y, Li J, Mei O, Zhong J, You W, Shen G, Wu X, Li J, Shu Y, Shi LL, Zhu Y, Reid RR, He TC, Fan J. Dermal fibroblast-derived extracellular matrix (ECM) synergizes with keratinocytes in promoting re-epithelization and scarless healing of skin wounds: Towards optimized skin tissue engineering. Bioact Mater. 2025; 47(1):1-17.
82. Jacob JA, Mahal HS, Biswas N, Mukherjee T, Kapoor S. Role of phenol derivatives in the formation of silver nanoparticles. Langmuir. 2008; 24(2):528-533.
83. Moond M, Singh S, Sangwan S, Devi R, Beniwal R. Green Synthesis and Applications of Silver Nanoparticles: A Systematic Review. AATCC J Res. 2022; 9(6):272-285.
84. Sarika Ankushrao N, Shilpa Pravin C. Biosynthesis of Silver Nanoparticles from Polyphenolic Extract of *Baliospermun solanifolium* using Central Composite Design. Pharmacog Res. 2022; 14(4):405-411.
85. Liu H, Chen L, Peng Y, Li X, Zhang H, Chen Y, Li Z, Dai F. A tea polyphenol-loaded cellulose/silk fibroin/polyacrylic acid hydrogel for wound healing. Cellulose. 2024; 31(13):8169-8187.
86. Tong MQ, Lu CT, Huang LT, Yang JJ, Yang ST, Chen HB, Xue PP, Luo LZ, Yao Q, Xu HL, Zhao YZ. Polyphenol-driven facile assembly of a nanosized acid fibroblast growth factor-containing coacervate accelerates the healing of diabetic wounds. Acta Biomater. 2023; 157:467-486.
87. Mehwish HM, Liu G, Rajoka MSR, Cai H, Zhong J, Song X, Xia L, Wang M, Aadil RM, Inam-Ur-Raheem M. Therapeutic potential of *Moringa oleifera* seed polysaccharide embedded silver nanoparticles in wound healing. Int J Biol Macromol. 2021; 184:144-158.
88. Galdopórpora JM, Ibar A, Tuttolomondo MV, Desimone MF. Dual-effect core–shell polyphenol coated silver nanoparticles for tissue engineering. Nano-Struct Nano-Objects. 2021; 26:100716.